

How Small Can 6G Reason? Scaling Tiny Language Models for AI-Native Networks

Mohamed Amine Ferrag^{*‡}, Abderrahmane Lakas^{*}, Merouane Debbah[†]

^{*} Department of Computer and Network Engineering, United Arab Emirates University, UAE

[†] Research Institute for Digital Future, Khalifa University, UAE

[‡] Corresponding author: mohamed.ferrag@uaeu.ac.ae

Abstract—Emerging 6G visions, reflected in ongoing standardization efforts within 3GPP, IETF, ETSI, ITU-T, and the O-RAN Alliance, increasingly characterize networks as AI-native systems in which high-level semantic reasoning layers operate above standardized control and data-plane functions. Although frontier-scale large language models (LLMs) such as Qwen2.5-7B and Olmo-3-7B demonstrate strong reasoning capability, their computational footprint limits deployment in latency-sensitive, edge-native infrastructures. This paper presents a systematic empirical study of the scaling behavior and deployment efficiency of compact language models for network-level semantic reasoning in AI-native 6G systems. Using 6G-Bench—a standardization-aligned benchmark comprising 30 decision-making tasks across five capability domains—we evaluate models ranging from 135M (SmolLM2-135M) to 7B parameters (Qwen2.5-7B), including mid-scale architectures such as Llama-3.2-1B, Granite-1B, and Qwen2.5-3B. Deterministic accuracy (pass@1) increases from 0.224 at 135M to 0.707 at 7B, but scaling gains are highly non-uniform. A pronounced stability transition occurs in the 1–1.5B range, where accuracy rises from 0.373 (Llama-3.2-1B) to 0.531 (Qwen2.5-1.5B) and the instability gap Δ_5 contracts from 0.356 to 0.138. Beyond 3B parameters, improvements diminish (+0.064 from 3B to 7B). Through single-query inference profiling and an Edge Score metric that normalizes accuracy by latency and memory footprint, we show that semantic reliability per unit edge resource does not scale monotonically with parameter count. Instead, mid-scale models (approximately 1.5–3B) achieve the most favorable balance between deterministic stability and computational efficiency, providing deployment-relevant guidance for AI-native 6G architectures. All scripts and results are publicly available at <https://github.com/maferrag/6G-Bench>.

Index Terms—6G, Small Language Models, Tiny LLMs, Semantic Communication, Network-Level Reasoning, AI-Native Networks, Scaling Analysis

I. INTRODUCTION

The evolution toward AI-native 6G networks represents a structural transformation in how intelligence is embedded into communication systems. Unlike previous generations, in which machine learning served localized optimization roles, 6G visions position artificial intelligence as a native architectural layer spanning radio access networks (RAN) [1], core networks, and distributed edge–cloud infrastructures. Within 3GPP [2], architectural evolution toward service-based systems, intent-driven management, network exposure functions (NEF), network slicing, and network digital twins reflects the emergence of semantic control layers operating above standardized protocol stacks. The O-RAN Alliance [3] advances intelligent RAN through near-real-time and non-real-time RIC

controllers enabling AI-driven closed-loop control, while ETSI MEC [4] formalizes edge-native orchestration. In parallel, IETF work [5] on intent-based networking, autonomous networks, and zero-trust architectures, together with ITU-T IMT-2030 frameworks [6], envisions networks capable of sub-millisecond latency (< 1 ms), peak data rates approaching 0.1–1 Tbps, reliability beyond 99.99999%, and pervasive AI integration. Achieving such targets requires real-time semantic reasoning under stringent compute, energy, and security constraints.

At the physical and system levels, 6G introduces disruptive technologies that dramatically increase network dimensionality and controllability. Operation in sub-THz and THz bands (100 GHz–1 THz), extremely large antenna arrays (ELAA) [7] with hundreds to thousands of elements, cell-free massive MIMO [8], and reconfigurable intelligent surfaces (RIS) comprising hundreds or thousands of programmable meta-elements enable programmable propagation environments [9]. Integrated Sensing and Communication (ISAC), semantic communication, distributed digital twins, native federated learning, and quantum-safe or quantum-assisted networking further couple communication, computation, and intelligence [10]. Emerging quantum technologies—including quantum key distribution (QKD), quantum random number generation, and early-stage quantum networking—introduce new trust and security paradigms, while quantum-enhanced optimization promises acceleration for combinatorial resource allocation [11]. Coordinating RIS phase shifts, THz beam alignment, slice arbitration across URLLC/eMBB/mMTC regimes, digital twin synchronization, and quantum-secure trust management requires multi-step reasoning across radio, compute, and policy layers. Large language models (LLMs) and AI agents are therefore being explored as semantic reasoning engines that can orchestrate these heterogeneous capabilities [12], [13]. However, frontier-scale LLMs typically range from 70B to 500B parameters, require hundreds of gigabytes of memory, and depend on multi-accelerator clusters—rendering them impractical for deployment at RAN nodes or MEC platforms with tight power and latency budgets.

This architectural tension intersects with classical scaling law research in large language models. Kaplan et al. demonstrated that language modeling loss follows a power-law with respect to model size, with exponent $\alpha_N \approx 0.076$, while compute-optimal scaling analyses such as Chinchilla [14] showed that optimal performance under fixed FLOPs

budgets requires near-equal scaling of parameters and tokens ($N \propto C^{0.5}$, $D \propto C^{0.5}$). Subsequent work on emergent abilities identified qualitative capability transitions beyond approximately 10^{22} – 10^{23} FLOPs, often corresponding to 10B–100B parameter regimes. These studies rely on log-linear regression, power-law fitting, and breakpoint detection to characterize smooth scaling or phase-transition behavior [15], [16]. Yet they primarily optimize cross-entropy loss or open-domain benchmark accuracy. In contrast, AI-native 6G systems impose fundamentally different constraints: deterministic single-shot reliability, bounded reasoning instability, strict adherence to zero-trust and quantum-safe security policies, and control-loop operation potentially below 1 ms. Whether similar scaling exponents, regime transitions, or saturation effects emerge in structured, safety-critical network reasoning—particularly within the compact 0.1B–7B parameter range suitable for edge deployment—remains unexplored.

This motivates a central question for AI-native 6G architecture design: *How does network-level semantic reasoning capability scale in small and tiny language models under 6G constraints?* Unlike conventional QA benchmarks, 6G decision-making requires structured reasoning across heterogeneous abstractions, including intent feasibility under dynamic network state, slice selection and resource arbitration, RIS and massive MIMO configuration, THz beam management, SLA violation forecasting, trust-aware compute exposure, quantum-secure authentication, inter-operator federation, distributed AI coordination, and ISAC-driven control. These capabilities align with architectural trajectories articulated in 3GPP service-based systems, IETF intent networking drafts [5], ETSI MEC orchestration frameworks [4], O-RAN intelligent control loops [3], and ITU IMT-2030 visions [6]. Determining whether stable deterministic reasoning emerges at 0.5B, 1B, or 3B parameters—and quantifying the marginal gains beyond this regime—therefore becomes not only a scaling-law investigation, but a foundational architectural problem for deploying AI agents across hierarchical 6G, edge, and quantum-enhanced network tiers.

In this work, we conduct a systematic scaling analysis of small and tiny language models (135M–7B parameters) using 6G-Bench [17], a standardization-aligned evaluation framework comprising 30 decision-making tasks organized into five capability domains derived from 3GPP, IETF, ETSI, ITU-T, and O-RAN architectural directions. Rather than proposing a new benchmark, we leverage this controlled evaluation environment to characterize empirical scaling regimes governing deterministic semantic reasoning in AI-native 6G contexts. Our study explicitly targets the deployment-relevant regime below 10B parameters—far smaller than frontier LLMs (70B–500B)—and focuses on safety-critical, policy-constrained network reasoning under zero-shot, deterministic decoding. We quantify how pass@1 accuracy evolves from 0.224 at 135M parameters to 0.707 at 7B, identify a pronounced stability transition in the 1–1.5B range, and analyze how reasoning instability (Δ) contracts from 0.365 to 0.031 as scale increases. This enables principled characterization of when compact LLM-based AI agents become sufficiently reliable for hierarchical 6G control-plane deployment.

A. Contributions

This paper makes the following contributions:

- **First systematic SLM scaling study for AI-native 6G semantic reasoning.** We evaluate 10 instruction-tuned models spanning 135M to 7B parameters across dense Transformer and hybrid architectures, using 6G-Bench’s 30 standardized tasks aligned with intent management, slicing, trust, agentic control, and distributed intelligence in 6G systems.
- **Identification of empirical scaling regimes and a stability threshold.** We demonstrate that scaling gains are highly non-uniform. Deterministic accuracy increases from 0.373 at 1B to 0.531 at 1.5B, marking a sharp transition in reasoning reliability. Beyond 3B parameters, marginal improvements diminish, with pass@1 improving by only 0.064 between 3B and 7B.
- **Deterministic stability analysis via pass@1, pass@k, and instability gap (Δ_k).** We formalize reasoning instability as $\Delta_k = A_k - A_1$ and show that the gap collapses from 0.356–0.383 in the sub-1B regime to 0.051 at 3B and 0.031 at 7B. This contraction indicates convergence between stochastic exploration and deterministic inference, a prerequisite for safety-critical control tasks in zero-trust, SLA-bound 6G environments.
- **Heterogeneous domain-level scaling elasticity characterization.** Using a log-parameter sensitivity coefficient SG_j , we quantify domain-specific scaling responsiveness. Intent & Policy Reasoning exhibits the highest elasticity ($SG_1 = 0.154$), while Trust, Security & SLA Awareness shows the lowest ($SG_3 = 0.104$). Distributed Intelligence & Emerging 6G Use Cases ($SG_5 = 0.131$) demonstrate strong scale dependence, reflecting the complexity of federated orchestration, ISAC coordination, and digital twin synchronization.
- **Deployment-tier implications for AI agents in hierarchical 6G architectures.** Grounded in empirical scaling regimes, inference profiling, and the proposed Edge Score, we map capability–efficiency trade-offs to realistic 6G deployment tiers: (i) ultra-compact models (≤ 350 M) for localized RAN/MEC advisory reasoning where resource efficiency dominates; (ii) mid-scale models (1.5–3B) that lie on the capability–efficiency frontier for stability-critical intent translation, agentic coordination, RIS/THz configuration logic, and cross-slice arbitration; and (iii) optional 7B-class models for centralized orchestration, where marginal robustness gains justify higher latency and memory cost.

The remainder of this paper is organized as follows. Section II reviews classical scaling laws for large language models and discusses their limitations in the context of safety-critical, AI-native 6G network reasoning. Section III presents the methodology, including the 6G-Bench task taxonomy, the evaluated model spectrum (135M–7B parameters), the experimental protocol, and the formal definitions of deterministic and stochastic stability metrics. Section IV provides the empirical scaling analysis, covering global performance trends, instability-gap contraction, domain-specific scaling elasticity,

TABLE I
COMPARISON OF SCALING STUDIES AND THEIR SCOPE RELATIVE TO AI-NATIVE 6G SEMANTIC REASONING.

Aspect	Kaplan et al. [15]	Hoffmann et al. [14]	Wei et al. [16]	This Work
Primary Objective	LM loss scaling	Compute-optimal LM	Emergent abilities	6G semantic reasoning
Evaluation Metric	Cross-entropy	Cross-entropy	Downstream accuracy	pass@1, pass@k, Δ_k
Scale Range	10^3 – 10^9	70M–280B	10B–500B	135M–7B
AI-Native 6G Task Alignment	✗	✗	✗	✓
Deterministic Stability Analysis	✗	✗	✗	✓
Domain-Specific Scaling Elasticity	✗	✗	✗	✓
Edge Deployment Focus	✗	✗	✗	✓

and deployment-tier implications for hierarchical 6G architectures. Section V concludes the paper and outlines directions for future research on compact LLM-based AI agents for edge-native, quantum-secure 6G systems.

II. RELATED WORK

Recent research on large language models has established strong empirical regularities governing performance as a function of model size, training data, and compute. Foundational studies have derived predictive power-law relationships for language modeling loss and compute-optimal allocation, while subsequent work has identified qualitative capability transitions at large scales. However, these analyses have primarily focused on open-domain NLP benchmarks and token-level objectives, leaving structured, safety-critical semantic reasoning in AI-native 6G network control settings largely unexplored. Table I presents a comparison of prior language model scaling studies and highlights their differences relative to AI-native 6G semantic reasoning requirements.

A. Scaling Laws for Large Language Models

Kaplan et al. [15] presented a systematic empirical investigation of scaling behavior in autoregressive Transformer language models, demonstrating that test cross-entropy loss follows remarkably stable power-law relationships with respect to model size, dataset size, and training compute. Using models ranging from approximately 10^3 to 10^9 non-embedding parameters and datasets spanning over two orders of magnitude, they showed that performance scales as $L(N) = (N_c/N)^{\alpha_N}$ with $\alpha_N \approx 0.076$ and $N_c \approx 8.8 \times 10^{13}$ parameters, when trained with sufficiently large data. Similarly, in the data-limited regime, loss follows $L(D) = (D_c/D)^{\alpha_D}$ with $\alpha_D \approx 0.095$ and $D_c \approx 5.4 \times 10^{13}$ tokens. When training is compute-constrained under optimal allocation, the loss scales as $L(C_{\min}) = (C_c^{\min}/C_{\min})^{\alpha_C^{\min}}$ with $\alpha_C^{\min} \approx 0.050$ and $C_c^{\min} \approx 3.1 \times 10^8$ PF-days. Importantly, they derived a unified formulation, $L(N, D)$, that captures overfitting behavior, showing that data requirements grow sublinearly with model size, with $D \propto N^{0.74}$ to maintain performance. The study further demonstrated that optimal compute allocation favors rapid growth in model size ($N \propto C_{\min}^{0.73}$), while training steps increase negligibly ($S_{\min} \propto C_{\min}^{0.03}$), implying that larger models are increasingly sample-efficient. Architectural hyperparameters such as depth and width were shown to have only weak effects compared to scale itself. While this work established a predictive scaling-law framework for language

modeling loss over eight orders of magnitude in compute, it focused exclusively on perplexity-based next-token prediction over web-scale corpora. It did not investigate the reliability of deterministic decision-making, policy-consistent reasoning, or structured semantic control tasks aligned with AI-native 6G architectures. In particular, the implications of scaling laws for safety-critical network-level reasoning, intent alignment, SLA-aware decision-making, and multi-agent coordination in 6G systems remain unaddressed, motivating the present study on scaling regimes for tiny and small language models in AI-native 6G networks.

B. Compute-Optimal Scaling and Data-Parameter Trade-offs

Hoffmann et al. [14] revisited the problem of compute-optimal scaling for large language models and challenged prior conclusions regarding the trade-off between parameter count and training data. Building on earlier scaling-law formulations, they empirically analyzed over 400 Transformer models ranging from 70M to 16B parameters and trained on 5B to 500B tokens, explicitly modeling the loss $L(N, D)$ under a fixed FLOPs constraint. In contrast to prior work suggesting that model size should grow faster than dataset size, they found that compute-optimal training requires scaling model parameters and training tokens in approximately equal proportions. Concretely, they estimated scaling exponents $N_{\text{opt}} \propto C^a$ and $D_{\text{opt}} \propto C^b$ with $a \approx 0.49$ – 0.50 and $b \approx 0.50$ – 0.51 , depending on the fitting methodology, in sharp contrast to Kaplan et al.’s prediction of $a = 0.73$ and $b = 0.27$. Their analysis demonstrated that many contemporary large models were substantially undertrained relative to their compute budgets. To validate this hypothesis, they trained the 70B-parameter *Chinchilla* model on 1.4 trillion tokens using the same compute budget as the 280B-parameter Gopher model trained on 300B tokens. Despite being four times smaller, *Chinchilla* uniformly outperformed Gopher across downstream evaluations, achieving 67.6% average accuracy on the MMLU benchmark—an improvement of more than 7%—while also reducing LM inference and fine-tuning costs. These findings established that optimal performance depends critically on a balanced scaling between model and dataset sizes under fixed compute. However, similar to prior scaling-law studies, the analysis was conducted exclusively on language modeling loss and downstream NLP benchmarks.

C. Emergent Abilities and Phase Transitions in Scaling

Wei et al. [16] presented a systematic analysis of what they term *emergent abilities* in large language models, describing

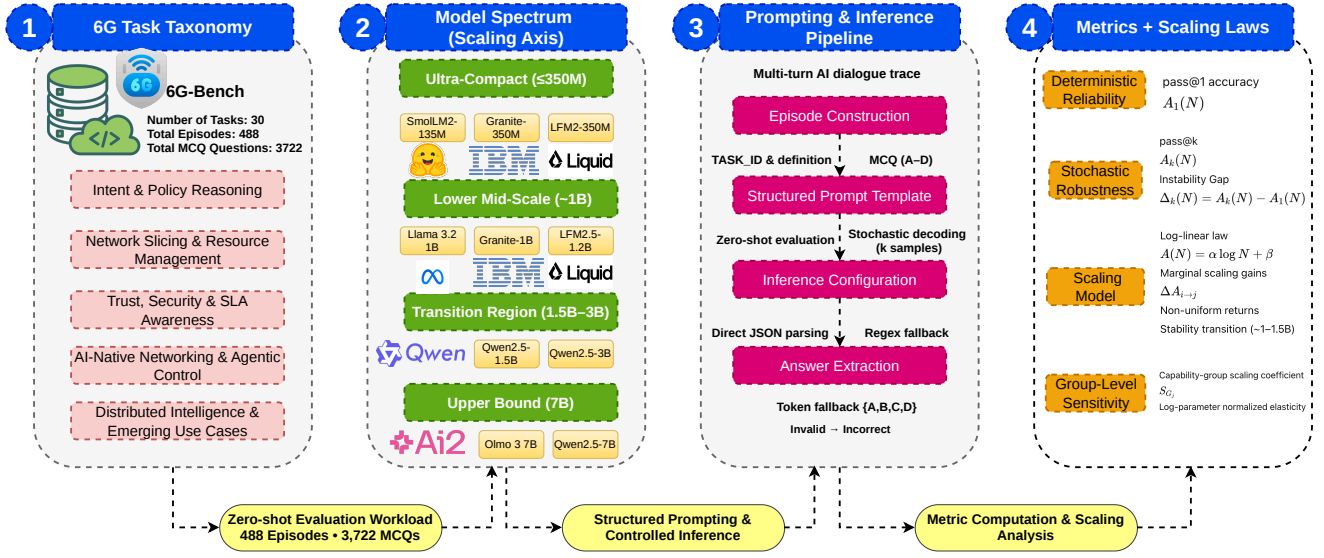


Fig. 1. End-to-End Methodological Framework for Evaluating Parameter Scaling and Semantic Reasoning Stability in 6G-Bench.

qualitative capability transitions that occur only beyond specific scale thresholds. An ability is defined as emergent if it is absent in smaller models but appears abruptly in larger ones, thereby violating smooth extrapolation from conventional scaling curves. Empirically, they demonstrated phase-transition-like behavior across multiple task families when plotting performance against training compute (FLOPs) or parameter count. For example, in modular arithmetic benchmarks, models trained below approximately 2×10^{22} FLOPs ($\approx 13B$ parameters) achieved near-random accuracy, whereas performance sharply increased beyond this threshold. Similarly, on the MMLU benchmark (57-task average), models below roughly 10^{22} FLOPs ($\approx 10B$ parameters) performed at chance level, while scaling to $3\text{--}5 \times 10^{23}$ FLOPs (70B–280B parameters) yielded substantial gains, with Chinchilla [14] and Gopher [18] achieving markedly higher accuracy. In the TruthfulQA benchmark, performance improvements were observed only at the largest scales ($\approx 5 \times 10^{23}$ FLOPs, 280B parameters). Additional emergent effects were reported for chain-of-thought prompting, instruction fine-tuning, scratchpad reasoning, calibration strategies, and multilingual reasoning, with emergence often occurring around the 10^{23} FLOP regime ($\approx 50B\text{--}100B$ parameters).

D. Limitations of Prior Scaling Studies for AI-Native 6G

Despite the substantial progress in understanding language model scaling, prior studies remain fundamentally centered on open-domain NLP objectives and token-level performance metrics. Kaplan et al. [15] and Hoffmann et al. [14] derive predictive power-law relationships for cross-entropy loss under varying parameter, data, and compute regimes, while Wei et al. [16] analyze qualitative capability transitions across downstream reasoning benchmarks. However, these works evaluate perplexity, few-shot accuracy, or prompting-based task performance rather than deterministic decision reliability under structured, safety-critical constraints. AI-native 6G

networks introduce distinct requirements: semantic reasoning must operate within latency constraints, adhere to policy enforcement rules, operate under partial observability, satisfy SLA constraints, and coordinate across heterogeneous domains. Tasks such as intent feasibility assessment, trust-aware compute exposure, slice arbitration, and distributed intelligence orchestration are not equivalent to standard NLP benchmarks and demand consistent single-shot correctness and stability under deterministic decoding. Furthermore, existing scaling analyses primarily focus on large-scale regimes (tens to hundreds of billions of parameters), leaving the sub-billion- to low-billion-parameter range—most relevant for edge-native deployment—largely uncharacterized in terms of semantic control reliability. Consequently, there is currently no empirical framework that examines scaling regimes, stability thresholds, and domain-specific scaling elasticity for structured network-level reasoning in AI-native 6G systems, motivating the dedicated small-model scaling analysis conducted in this work.

III. METHODOLOGY

This section describes the experimental framework used to evaluate the scaling behavior of small and mid-scale language models for network-level semantic reasoning in AI-native 6G systems. We first present the task taxonomy and capability grouping underlying 6G-Bench, followed by the evaluated model spectrum spanning 135M to 7B parameters. We then detail the structured prompting protocol, the construction of the dataset, the inference configuration, and the reproducibility controls used for zero-shot evaluation across 488 episodes and 3,722 multiple-choice questions. Finally, we formalize deterministic and stochastic evaluation metrics, introduce the instability gap, and define log-linear and group-level scaling models used to characterize parameter-dependent reasoning regimes. Fig. 1 presents the complete experimental framework

for evaluating scaling-dependent semantic reasoning in AI-native 6G systems.

A. Task Taxonomy and Capability Groups

The 6G-Bench benchmark [17] defines 30 decision-making tasks (T1–T30) organized into five capability-aligned categories derived from ongoing standardization efforts in 3GPP, IETF, ETSI, ITU-T, and the O-RAN Alliance. The five capability groups are:

- **Intent & Policy Reasoning:** semantic consistency under evolving network state and policy constraints.
- **Network Slicing & Resource Management:** slice selection, compute placement, SLA forecasting, and resource arbitration.
- **Trust, Security & SLA Awareness:** trust-aware exposure, authorization reasoning, and automated security response.
- **AI-Native Networking & Agentic Control:** inter-agent coordination, federation, lifecycle management, and task offloading.
- **Distributed Intelligence & Emerging Use Cases:** federated learning orchestration, Integrated Sensing and Communication (ISAC), digital twins, and public-safety coordination.

1) *Task Formatting, Answer Extraction, and Grading Protocol:* Each evaluation instance consists of a structured episode–question pair. Episodes are stored as JSON objects containing (i) an initial system state (environment, airspace, UAV configuration, and policy constraints), and (ii) a multi-turn dialogue trace including intents, actions, network telemetry, and tool responses. For each episode, one or more multiple-choice questions (MCQs) are defined, each associated with a task identifier (T1–T30), four answer options (A–D), a ground-truth label, and metadata including the source turn and difficulty.

To ensure controlled reasoning and reproducible grading, the model is prompted using a structured template comprising:

- Target task identifier and task definition,
- A summarized episode context,
- The MCQ question text,
- Four labeled answer options (A–D), and
- A strict output instruction requiring valid JSON of the form `{"answer": "A"}`.

The episode summary is programmatically generated to include:

- Initial environmental, airspace, UAV, and policy context,
- Mission success indicator,
- A truncated dialogue trace (up to 12 turns), and
- Aggregated network telemetry per turn (slice, latency, jitter, loss, throughput, edge load).

The model must return a single JSON object. Output parsing follows a deterministic extraction pipeline: (i) attempt direct JSON parsing; (ii) if parsing fails, apply regular-expression-based extraction of the `"answer"` field; and (iii) as a fallback, extract a standalone token in `{A, B, C, D}`. A prediction is considered valid only if it resolves to one of the four options; all other outputs are marked as incorrect.

B. Model Spectrum and Experimental Protocol

To systematically characterize the scalability of semantic reasoning under AI-native 6G constraints, we evaluate a diverse set of compact and mid-scale language models ranging from 135M to 7B parameters. The selected models represent multiple architectural paradigms, training regimes, and deployment targets, allowing controlled analysis of both parameter scaling effects and architectural efficiency. Table II summarizes the evaluated model spectrum, detailing parameter scale, organizational origin, architectural design, alignment strategy, and deployment orientation.

1) *Model Selection Rationale:* The model spectrum was constructed to satisfy four methodological objectives: (i) granular coverage of the sub-1B regime, where edge-native deployment is most realistic; (ii) dense sampling of the 1–1.5B transition region, hypothesized to represent a stability boundary; (iii) inclusion of mid-scale (3B) and upper-bound (7B) models to identify diminishing returns; and (iv) architectural heterogeneity, including conventional dense Transformer models and hybrid convolution-attention designs optimized for edge inference. All evaluated models are instruction-tuned variants, reflecting the intent-driven and policy-conditioned nature of 6G semantic reasoning tasks.

2) *Ultra-Compact Regime ($\leq 350M$ Parameters):*

a) *SmolLM2-135M:* SmolLM2-135M [19] represents the extreme edge-deployable regime. Despite its compact size, the model is trained on approximately two trillion tokens using a diversified corpus that includes educational data, code repositories, and curated high-quality text sources. Instruction alignment is achieved via supervised fine-tuning followed by Direct Preference Optimization, improving robustness under structured prompts. This model provides a lower bound on semantic reasoning capability under strict parameter and memory constraints.

b) *Granite-4.0-350M:* Granite-350M [20] is a lightweight, instruction-tuned model developed by IBM and derived from a base checkpoint via supervised instruction tuning, reinforcement learning, and model merging. It is explicitly designed for on-device deployment and domain adaptation with limited computational overhead. Its inclusion allows examination of alignment-enhanced dense Transformers at the sub-500M scale.

c) *LFM2-350M:* LFM2-350M [21] introduces architectural diversity into the ultra-compact regime. Unlike purely Transformer-based designs, it employs a hybrid Liquid architecture incorporating multiplicative gating mechanisms and short convolutional blocks. This design prioritizes training efficiency and low-latency inference on CPU, GPU, and NPU hardware. Including LFM2 enables assessment of whether architectural innovation can partially offset limited parameter capacity in structured network reasoning tasks.

3) *Lower Mid-Scale Regime ($\approx 1B$ Parameters):*

a) *Llama 3.2 1B Instruct:* Llama 3.2 1B Instruct [22] provides a widely adopted dense-Transformer baseline at the 1B scale. Optimized for efficient multilingual instruction following and low-resource deployment, it serves as a reference model for evaluating the reliability of deterministic reasoning near the hypothesized scaling transition.

TABLE II
EVALUATED MODEL SPECTRUM ACROSS PARAMETER SCALE, ORGANIZATION, ARCHITECTURE, AND ALIGNMENT PIPELINE. ALL MODELS WERE DOWNLOADED FROM HUGGING FACE AND EVALUATED LOCALLY UNDER A UNIFIED INFERENCE PROTOCOL.

Model	Organization	Params (B)	Architecture	Alignment	Context	Target Deployment	Ref.
SmolLM2-135M	Hugging Face	0.135	Dense Transformer	SFT + DPO	8K	Ultra-edge	[19]
Granite-4.0-350M	IBM	0.35	Dense Transformer	SFT + RL + Merge	8K	On-device	[20]
LFM2-350M	Liquid AI	0.35	Hybrid (Conv + Attn)	Post-train	8K	Edge CPU/NPU	[21]
Llama 3.2 1B	Meta	1.0	Dense Transformer	Instruct SFT	8K	Edge/Control	[22]
Granite-4.0-H-1B	IBM	1.0	Dense Transformer	SFT + RL	8K	Domain-adaptive	[20]
LFM2.5-1.2B	Liquid AI	1.2	Hybrid (LIV + GQA)	Ext. Pretrain + RL	32K	Edge long-context	[21]
Qwen2.5-1.5B	Alibaba	1.5	Dense (RoPE, SwiGLU)	Pretrain + Post	32K	Control-plane	[23], [24]
Qwen2.5-3B	Alibaba	3.0	Dense (RoPE, SwiGLU)	Pretrain + Post	32K	Operator domain	[23], [24]
Olmo 3 7B	AI2	7.0	Dense Transformer	Instruct SFT	8K	Central control	[25]
Qwen2.5-7B	Alibaba	7.0	Dense (RoPE, SwiGLU)	Pretrain + Post	32K	Central orchestration	[23], [24]

Abbreviations: SFT = Supervised Fine-Tuning; RL = Reinforcement Learning; DPO = Direct Preference Optimization; Merge = Model Merging; Conv = Convolution; Attn = Attention; LIV= linear input-varying operators; GQA = Grouped-Query Attention; RoPE = Rotary Positional Embedding; SwiGLU = Swish-Gated Linear Unit; Pretrain = Pre-training; Post = Post-training alignment.

b) *Granite-4.0-H-1B*: Granite-4.0-H-1B [20] extends the Granite nano family into the billion-parameter regime while retaining its reinforcement-learning-enhanced alignment pipeline. Its inclusion enables controlled comparison between dense Transformer families at similar parameter scale, isolating architectural and training effects from raw capacity growth.

c) *LFM2.5-1.2B-Instruct*: LFM2.5-1.2B [21] represents an architectural evolution of the hybrid Liquid design. It combines convolutional LIV blocks with grouped-query attention layers and is trained on an extended 28-trillion-token corpus. The model supports long-context reasoning (up to 32K tokens) while maintaining a memory footprint compatible with edge devices. This model is particularly relevant for analyzing whether hybrid architectures can shift the deterministic stability transition downward relative to conventional Transformers.

4) Mid-Scale and Upper-Bound Regime (1.5B–7B):

a) *Qwen2.5-1.5B-Instruct*: Qwen2.5-1.5B [23], [24] marks the lower boundary of the empirically observed stability transition. Architecturally, it employs rotary positional embeddings, SwiGLU activations, RMS normalization, and grouped-query attention. The model is optimized for structured output generation, long-context reasoning, and multilingual robustness. Its role in the study is central for identifying the onset of deterministic reasoning consistency.

b) *Qwen2.5-3B-Instruct*: The 3B variant increases depth and attention capacity while preserving architectural design. It enables evaluation of whether scaling beyond the transition region yields qualitative reasoning improvements or primarily incremental refinement [23], [24].

c) *Olmo 3 7B Instruct*: Olmo 3 7B Instruct [25] is a supervised, instruction-tuned dense Transformer trained under an open, transparent training pipeline. It serves as an upper-bound dense baseline within the compact-large regime, providing insight into performance saturation at higher parameter scales.

d) *Qwen2.5-7B-Instruct*: Qwen2.5-7B [23], [24] represents the largest model in our evaluation and provides an empirical ceiling for deterministic semantic reasoning under the 6G-Bench workload. Its inclusion allows precise quantification of diminishing marginal returns relative to the 3B regime.

Across the spectrum, the evaluated models span two principal architectural classes: dense Transformer architectures

(Llama, Granite, Qwen, Olmo) and hybrid Liquid architectures (LFM2 family) integrating convolutional processing with gated attention mechanisms. This diversity enables separating pure parameter-scaling effects from architectural-efficiency and alignment contributions.

All models were evaluated locally without reliance on external APIs. Each checkpoint was downloaded from Hugging Face and executed in a controlled inference environment to ensure reproducibility, uniform decoding configurations, and consistent hardware conditions. No additional fine-tuning was performed on 6G-Bench tasks; all results reflect zero-shot semantic reasoning under deployment-realistic constraints.

The selected spectrum mirrors realistic 6G deployment tiers: ultra-compact models ($\leq 350M$) targeting embedded RAN and edge nodes; 1–1.5B models suitable for control-plane semantic reasoning under moderate resource budgets; 3B models representing high-stability operator-domain reasoning; and 7B models approximating centralized orchestration layers. This structured selection enables identification of scale-dependent stability regimes and provides deployment-grounded guidance for integrating compact semantic reasoning layers into AI-native 6G architectures.

C. Prompt Template and Context Conditioning Protocol

For models that support chat formatting, the native tokenizer function `apply_chat_template` is used to construct the input prompt. For other models, a structured system–user concatenation is employed.

The system message defines the evaluator role, e.g.,

System Prompt

You are an expert 6G network AI agent evaluator. You will answer a multiple-choice question (A/B/C/D) about a UAV mission episode. Use the episode context and the target task definition to choose the best answer. You *must* respond with a single JSON object of the form `{"answer": "A"}`.

The user message contains:

- `TASK_ID`, `TASK_NAME`, and the formal task definition,

- The automatically generated episode summary,
- The MCQ question text,
- Options A–D, formatted as A: . . . , B: . . . , etc.,
- A strict instruction to respond only with JSON of the form {"answer": "A/B/C/D"}.

This uniform prompting protocol ensures that differences in performance arise from model capability and scale rather than prompt variation. Therefore, episode–question pairs are constructed by matching `.episode.json` files with their corresponding `.mcq.json` files in the dataset directory. Only episodes that have both files are included in the evaluation.

D. Evaluation Metrics and Stability Measures

Let $\mathcal{T} = \{t_1, \dots, t_M\}$ denote the evaluation task set, and let y_i^* be the ground-truth decision for task t_i . For a model with parameter scale N , let $\hat{y}_i^{(j)}(N)$ denote the j -th generated response under stochastic decoding.

a) *Deterministic Accuracy (pass@1)*: Under deterministic decoding (e.g., greedy decoding or temperature = 0), each task yields a single prediction $\hat{y}_i(N)$. We define deterministic single-shot accuracy as

$$A_1(N) = \frac{1}{M} \sum_{i=1}^M \mathbf{1}[\hat{y}_i(N) = y_i^*], \quad (1)$$

where $\mathbf{1}[\cdot]$ denotes the indicator function. This metric reflects safety-critical decision reliability under a single, policy-consistent inference trajectory. Since $A_1(N)$ is a binomial proportion over M MCQs, we report 95% confidence intervals using the normal approximation $A_1 \pm 1.96\sqrt{A_1(1 - A_1)/M}$.

b) *Stochastic Robustness (pass@k)*: Under stochastic decoding, each task produces k independent samples $\{\hat{y}_i^{(1)}(N), \dots, \hat{y}_i^{(k)}(N)\}$. We define pass@k as

$$A_k(N) = \frac{1}{M} \sum_{i=1}^M \mathbf{1}[\exists j \in \{1, \dots, k\} \text{ such that } \hat{y}_i^{(j)}(N) = y_i^*], \quad (2)$$

which quantifies the probability that at least one reasoning trajectory among k stochastic samples recovers the correct decision.

c) *Reasoning Instability*: To characterize stochastic inconsistency, we define the instability gap

$$\Delta_k(N) = A_k(N) - A_1(N), \quad (3)$$

which measures the extent to which correct reasoning exists but is not reliably selected under deterministic decoding. Confidence intervals for Δ_k are conservatively estimated by summing the variances of A_k and A_1 , yielding slightly wider but statistically safe uncertainty bounds.

All evaluations employ a standardized task-conditioned prompting protocol with robust answer extraction to ensure comparability across models.

1) *Log-Linear Scaling Model*: Let N denote the number of model parameters (in billions), and define $A(N) := A_1(N)$ as deterministic accuracy. To characterize scaling behavior, we approximate performance as a log-linear function of model size:

$$A(N) = \alpha \log(1 + N) + \beta + \epsilon(N), \quad (4)$$

where $\log(\cdot)$ denotes the natural logarithm. The inclusion of $1 + N$ stabilizes the transformation in the ultra-compact regime ($N \ll 1$), where $\log N$ becomes strongly negative.

where α captures the marginal improvement in semantic reasoning per logarithmic increase in parameter count, β is a baseline offset, and $\epsilon(N)$ represents architecture-dependent deviations.

The coefficients α and β are estimated via ordinary least squares (OLS) over all evaluated models. Residuals reported in Table IV are computed as $A_1 - (\alpha \log(1 + N) + \beta)$.

To quantify discrete scaling gains, we define

$$\Delta A_{i \rightarrow j} = A(N_j) - A(N_i). \quad (5)$$

Statistical comparisons between scales (e.g., 1B \rightarrow 1.5B) are performed using two-proportion z-tests on A_1 , with significance assessed at $\alpha = 0.05$.

Empirically, we observe that

$$\Delta A_{1B \rightarrow 1.5B} \gg \Delta A_{3B \rightarrow 7B}, \quad (6)$$

indicating non-uniform marginal returns and the presence of distinct scaling regimes rather than smooth proportional growth.

2) *Group-Level Scaling Sensitivity*: To quantify scaling elasticity across semantic capability domains, we define a group-level sensitivity coefficient for each capability group G_j :

$$S_{G_j} = \frac{\bar{A}_{G_j}(N_{\max}) - \bar{A}_{G_j}(N_{\min})}{\log(N_{\max}) - \log(N_{\min})}, \quad (7)$$

where $\bar{A}_{G_j}(N)$ denotes the mean deterministic accuracy (pass@1) across all tasks in group G_j at parameter scale N .

This coefficient estimates the average improvement in domain-specific semantic reasoning performance per logarithmic increase in model scale. By normalizing gains in log-parameter space, S_{G_j} enables direct comparison of scaling responsiveness across heterogeneous capability classes.

3) *Edge-Oriented Efficiency Metric*: While the preceding metrics characterize semantic reliability and scaling behavior, practical deployment in AI-native 6G systems also requires joint consideration of inference latency and memory footprint under edge constraints.

Let $L(N)$ denote the mean single-query inference latency (ms), and let $M(N)$ denote the mean peak VRAM usage (GB) for a model of scale N . To quantify semantic reliability per unit edge resource, we define the *Edge Score*:

$$ES(N) = \frac{A_1(N)}{L(N) \cdot M(N)}. \quad (8)$$

This metric jointly captures:

TABLE III
EXPERIMENTAL CONFIGURATION AND 6G-BENCH MCQ DATASET STATISTICS.

Component	Configuration / Value
Hardware Configuration	
GPUs	8 × NVIDIA A100 (80GB VRAM each)
Framework	PyTorch + Hugging Face Transformers
Precision	bfloat16 (CUDA), float32 (CPU fallback)
Device Placement	device_map="auto"
Quantization	None
Fine-Tuning	None (zero-shot evaluation)
Model Parameter Range	0.135B – 8.34B
Number of Models	11
Decoding Configuration	
Deterministic Decoding	Temperature = 0.0, do_sample = False
Stochastic Decoding	Temperature = 0.7, do_sample = True
Evaluation Metrics	pass@1 (deterministic), pass@3, pass@5 (stochastic)
Pass@k Values	$k \in \{3, 5\}$
Tasks with Pass@k	7 (T2, T9, T12, T19, T20, T26, T30)
Max New Tokens	Up to 10,000 (bounded by context window)
Seed Control	SHA-256 deterministic seed derivation
Inference Profiling Configuration	
Queries per Model	$R = 20$ runs (single-query profiling)
Prompt Length	2049 input tokens
Generated Tokens	8 output tokens (deterministic decoding)
FLOPs Estimation	Forward-pass FLOPs/query (TF) per model
6G-Bench MCQ Dataset Statistics	
Number of Tasks	30 (T1–T30)
Capability Groups	5 (G1–G5)
Total Episodes	488
Total MCQ Questions	3,722
Avg. MCQ per Episode	7.63
CI Estimation	95% binomial CI over $M = 3,722$ MCQs
Evaluation Setting	Strict JSON-constrained MCQ

- deterministic semantic accuracy (A_1),
- time-to-decision (L),
- and memory footprint (M).

Higher $ES(N)$ indicates greater semantic reliability per unit latency and memory cost, making it directly interpretable as an edge deployment efficiency measure. Unlike purely accuracy-based metrics, the Edge Score explicitly penalizes models that achieve marginal capability gains at the cost of disproportionately higher inference latency or memory overhead. It therefore provides a deployment-aware efficiency frontier that complements the scaling-law analysis.

IV. EMPIRICAL SCALING ANALYSIS

Table III summarizes the complete experimental configuration and dataset statistics used in this study. All evaluations were conducted on a multi-GPU server equipped with eight NVIDIA A100 GPUs (8×80GB VRAM), enabling stable zero-shot inference for models up to 7B parameters without quantization or parameter offloading. Deterministic (pass@1) and stochastic (pass@k) decoding regimes were implemented under strictly controlled seed management to ensure reproducibility. The evaluation corpus comprises 488 episodes and 3,722 multiple-choice questions spanning 30 capability-aligned tasks in 6G-Bench, yielding an average of 7.63 questions per episode. Seven tasks were additionally evaluated under pass@3 and pass@5 to quantify robustness to stochastic reasoning.

A. Global Scaling Trends: Deterministic and Stochastic Performance

Table IV presents deterministic single-shot accuracy (A_1), stochastic robustness (A_3, A_5), the instability gap (Δ_5), and log-scale efficiency ($\eta(N)$) for compact language models spanning 135M to 7B parameters. We additionally report 95% confidence intervals for A_1 and Δ_5 computed over $M = 3,722$ MCQs. Deterministic accuracy increases monotonically with scale, rising from 0.224 at 135M to 0.707 at 7B. However, the marginal gains are distinctly non-uniform: the transition from sub-1B to mid-scale models yields substantially larger improvements than the progression from 3B to 7B. In particular, the increase from 1B ($A_1 = 0.373$, 95% CI [0.357, 0.389]) to 1.5B ($A_1 = 0.531$, 95% CI [0.515, 0.547]) exhibits non-overlapping confidence intervals, and a two-proportion z-test yields $z \approx 13.9$ ($p \ll 0.001$), confirming that the observed jump is statistically significant. This concentration of gains in the 1–1.5B region indicates diminishing returns in the high-capacity regime and suggests the presence of empirical scaling regimes rather than smooth proportional growth. In effect, mid-scale models mark a qualitative shift in deterministic reasoning capability, while further scaling primarily delivers incremental refinement. The contraction of the instability gap $\Delta_5 = A_5 - A_1$ further clarifies this transition. In the low-capacity regime, large gaps (e.g., 0.365 at 135M) indicate that correct reasoning trajectories often exist but are not consistently selected under deterministic decoding. As model scale increases, Δ_5 collapses sharply—falling below 0.1 at 3B and reaching 0.031 at 7B—signaling convergence between stochastic exploration and deterministic inference. This stability transition reflects structural alignment between the model’s highest-probability trajectory and the correct reasoning path, a property essential for safety-critical network control. Beyond this regime boundary, additional scaling enhances robustness margins but does not fundamentally alter reasoning consistency, highlighting a critical trade-off between model capacity and deployment efficiency in AI-native 6G systems.

Using the fitted log-linear model $A(N) = \alpha \log(1+N) + \beta$, we analyze residuals to identify architecture-dependent deviations from pure parameter scaling. Models with positive residuals lie above the predicted scaling curve, indicating stronger-than-expected deterministic performance relative to their parameter count. Notably, Granite-1B exhibits the largest positive residual, followed by Qwen-3B and Qwen-1.5B, suggesting that alignment strategy and architectural design contribute measurable gains beyond raw parameter growth. In contrast, Llama-3.2-1B and Olmo-7B fall below the fitted trend, indicating slightly weaker performance relative to scale-based expectations. These deviations confirm that while parameter count explains the dominant performance trend, alignment pipelines and training corpus composition introduce systematic second-order effects.

B. Capability-Level Results

Complete per-task results (T1–T30), including model responses, task-level pass@1 accuracies, and full evaluation logs for all models, are publicly available in our accompanying

TABLE IV
SCALING ANALYSIS OF SMALL LANGUAGE MODELS ON 6G-BENCH.

Model	N (B)	$\log(1+N)$	A_1	95% CI (A_1)	A_3	A_5	Δ_5	95% CI (Δ_5)	$\eta(N)$	Residual
SmolLM2-135M	0.135	0.127	0.224	[0.210, 0.238]	0.440	0.589	0.365	[0.344, 0.386]	1.764	-0.026
Granite-350M	0.35	0.300	0.372	[0.356, 0.388]	0.606	0.755	0.383	[0.362, 0.404]	1.240	+0.015
LFM2-350M	0.35	0.300	0.358	[0.343, 0.374]	0.574	0.714	0.356	[0.334, 0.378]	1.193	+0.001
Llama-3.2-1B	1.0	0.693	0.373	[0.357, 0.389]	0.603	0.729	0.356	[0.334, 0.378]	0.538	-0.105
Granite-1B	1.0	0.693	0.559	[0.543, 0.575]	0.704	0.776	0.217	[0.196, 0.238]	0.806	+0.081
LFM2.5-1.2B	1.2	0.788	0.530	[0.514, 0.546]	0.606	0.676	0.146	[0.125, 0.167]	0.673	+0.009
Qwen-1.5B	1.5	0.916	0.531	[0.515, 0.547]	0.627	0.669	0.138	[0.117, 0.159]	0.580	+0.001
Qwen-3B	3.0	1.386	0.643	[0.628, 0.658]	0.678	0.694	0.051	[0.035, 0.067]	0.464	+0.006
Olmo-7B	7.0	2.079	0.652	[0.637, 0.667]	0.703	0.724	0.072	[0.055, 0.089]	0.314	-0.065
Qwen-7B	7.0	2.079	0.707	[0.692, 0.722]	0.730	0.738	0.031	[0.018, 0.044]	0.340	-0.010

Notation: N denotes the number of model parameters measured in billions (B). A_1 represents deterministic single-shot accuracy (pass@1). 95% confidence intervals for A_1 are computed using a binomial approximation over $M = 3,722$ MCQs. A_3 and A_5 represent stochastic success probabilities over three and five samples (pass@3 and pass@5), respectively. $\Delta_5 = A_5 - A_1$ denotes the reasoning instability gap. Confidence intervals for Δ_5 are conservatively estimated via variance summation of A_1 and A_5 . $\eta(N) = A_1 / \log(1+N)$ denotes log-scale reasoning efficiency. Residual denotes $A_1 - (\alpha \log N + \beta)$ with fitted coefficients $\alpha = 0.115$, $\beta = 0.478$.

TABLE V
GROUP-LEVEL SCALING SENSITIVITY S_{G_j} BETWEEN THE SMALLEST (SMOLLM2-135M, $N_{\min} = 0.135$ B) AND LARGEST (QWEN2.5-7B, $N_{\max} = 7$ B) MODELS. $\bar{A}_{G_j}(N)$ DENOTES MEAN PASS@1 OVER ALL TASKS IN GROUP G_j .

Group G_j	$\bar{A}_{G_j}(N_{\min})$	$\bar{A}_{G_j}(N_{\max})$	S_{G_j}
G1 – Intent & Policy Reasoning	0.174	0.782	0.154
G2 – Network Slicing & Resource Management	0.250	0.695	0.113
G3 – Trust, Security & SLA Awareness	0.268	0.679	0.104
G4 – AI-Native Networking & Agentic Control	0.209	0.683	0.120
G5 – Distributed Intelligence & Emerging 6G Use Cases	0.181	0.699	0.131

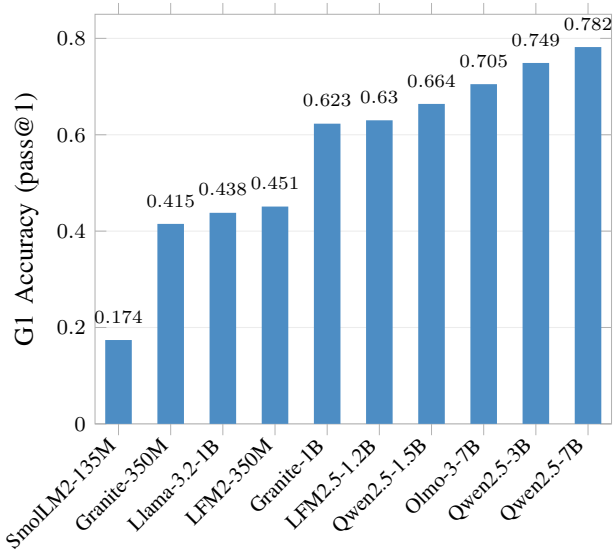


Fig. 2. Group G1 (Intent & Policy Reasoning): pass@1 accuracy across model scales.

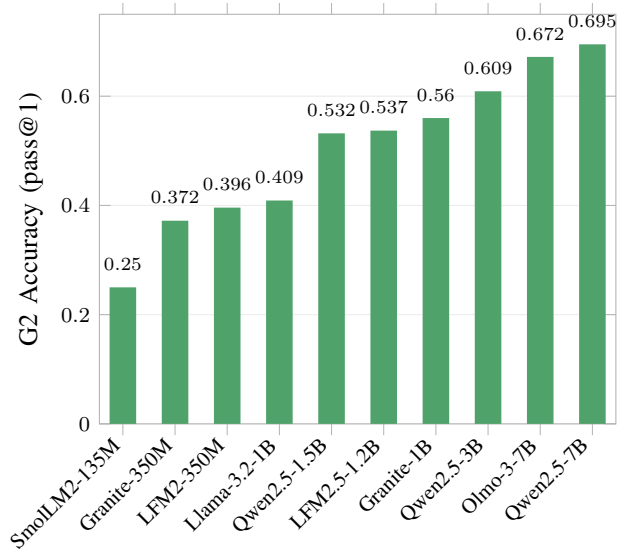


Fig. 3. Group G2 (Network Slicing & Resource Management): pass@1 accuracy across model scales.

GitHub repository. Due to space constraints, we report aggregated and group-level analyses in our paper.

1) *G1 – Intent & Policy Reasoning*: Figure 2 presents the pass@1 accuracy for Group G1 (Intent & Policy Reasoning), capturing models’ ability to perform multi-step intent interpretation, constraint alignment, and policy-consistent decision synthesis. A clear capacity-driven hierarchy emerges: Qwen2.5-7B achieves the highest accuracy (0.782), followed by Qwen2.5-3B (0.749) and Olmo-3-7B (0.705), indicating

that both parameter scale and architectural efficiency contribute to performance in intent-centric reasoning. Notably, the 3B Qwen variant approaches 7B-level performance, suggesting strong parameter utilization efficiency. In contrast, sub-billion-parameter models exhibit pronounced degradation, with Llama-3.2-1B (0.438) and SmolLM2-135M (0.174) demonstrating substantial reasoning collapse under policy consistency constraints. The nearly fourfold improvement from 135M to 7B underscores the strong dependence of intent

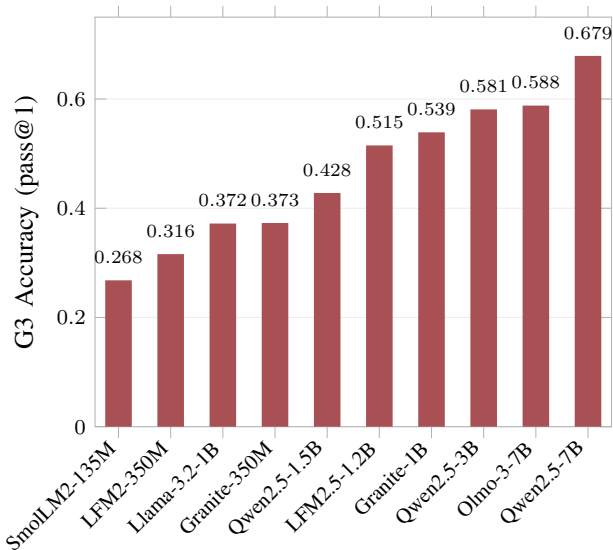


Fig. 4. Group G3 (Trust, Security & SLA Awareness): pass@1 accuracy across model scales.

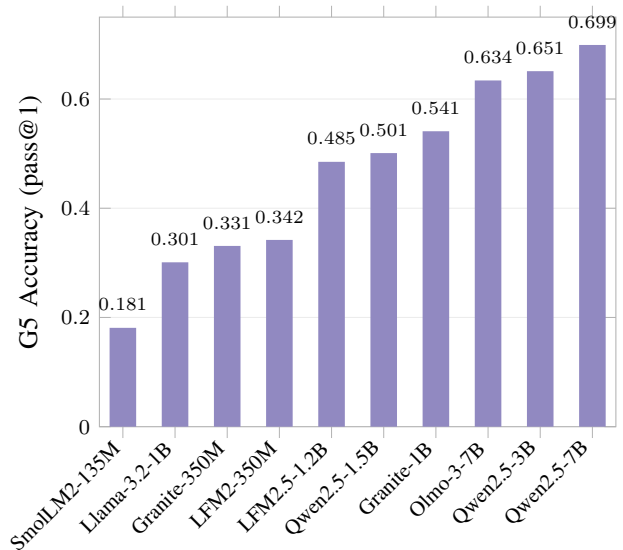


Fig. 6. Group G5 (Distributed Intelligence & Emerging 6G Use Cases): pass@1 accuracy across model scales.

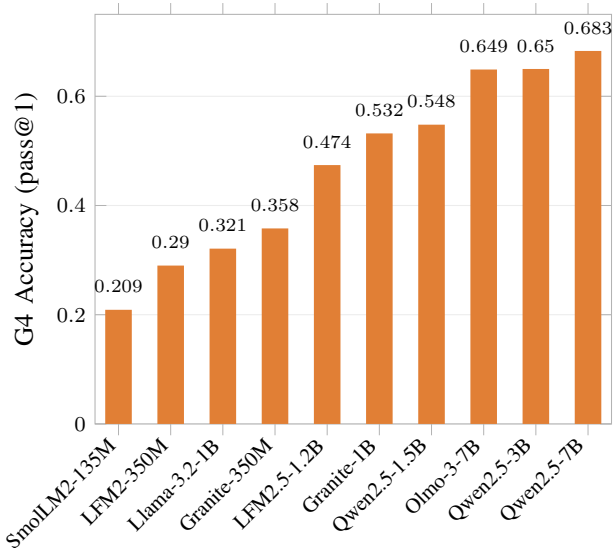


Fig. 5. Group G4 (AI-Native Networking & Agentic Control): pass@1 accuracy across model scales.

alignment and uncertainty-aware reasoning on representational capacity, indicating that policy-consistent semantic abstraction is intrinsically scale-sensitive.

2) *G2 – Network Slicing & Resource Management*: Figure 3 presents the results for Group G2 (Network Slicing & Resource Management), reflecting structured resource allocation, constraint satisfaction, and cross-layer optimization reasoning. While performance scales monotonically with parameter count, the gradient is less steep than in G1. Qwen2.5-7B leads (0.695), closely followed by Olmo-3-7B (0.672), suggesting that structured allocation reasoning benefits from scale but exhibits earlier saturation dynamics. The gap between 7B and 3B models is comparatively narrow, implying that slicing-related reasoning relies partially on structured constraint modeling rather than exclusively on deep latent abstrac-

tion. Sub-1B models retain moderate capability (0.40–0.56 range), indicating that these tasks remain partially tractable under constrained parameterization. Overall, G2 demonstrates steady yet comparatively moderate scaling behavior characteristic of semi-structured optimization domains.

3) *G3 – Trust, Security & SLA Awareness*: Figure 4 presents the pass@1 performance for Group G3 (Trust, Security & SLA Awareness), which emphasizes compliance verification, risk assessment, and service-level reasoning under adversarial or contractual constraints. The highest accuracy is obtained by Qwen2.5-7B (0.679), yet the relative improvement over mid-scale models such as Qwen2.5-3B (0.581) is less pronounced than in G1. LiquidAI LFM2.5-1.2B (0.515) performs competitively with several larger counterparts, suggesting that structured policy conditioning and the composition of training data may partially compensate for parameter scale in trust-oriented tasks. Although degradation toward ultra-small models remains evident (SmolLM2-135M at 0.268), the decline is comparatively smoother than in G1. This pattern indicates lower scaling elasticity and suggests that trust and SLA reasoning may saturate earlier with scale, potentially reflecting a stronger dependence on structured rule internalization than on increasingly deep generative abstraction.

4) *G4 – AI-Native Networking & Agentic Control*: Figure 5 presents the results for Group G4 (AI-Native Networking & Agentic Control), capturing sequential decision-making, autonomous orchestration, and control-loop reasoning. The top-performing models—Qwen2.5-7B (0.683), Qwen2.5-3B (0.650), and Olmo-3-7B (0.649)—form a tightly clustered high-performance regime, indicating that agentic control benefits from both scale and architectural design. The moderate performance gap between 7B and 3B models suggests diminishing marginal returns at higher capacity, possibly reflecting partial saturation in control-sequence abstraction. However, a pronounced drop occurs below the 1B threshold (e.g., Llama-3.2-1B at 0.321), highlighting the importance of

sufficient internal state representation for coherent multi-step orchestration. Performance dispersion across smaller models further suggests sensitivity to instruction-tuning and alignment mechanisms in agentic reasoning contexts.

5) *G5 – Distributed Intelligence & Emerging 6G Use Cases*: Figure 6 presents the pass@1 accuracy for Group G5 (Distributed Intelligence & Emerging 6G Use Cases), encompassing federated coordination, Integrated Sensing and Communication (ISAC), and digital twin synchronization. Scaling effects are again pronounced: Qwen2.5-7B achieves 0.699, whereas the smallest model attains only 0.181. The 3B variant (0.651) demonstrates strong parameter efficiency; however, the absolute improvement across scales remains substantial, indicating that distributed reasoning and cross-entity coordination impose significant representational demands. Compared to G2 and G3, where structured constraints partially mitigate scale limitations, G5 tasks appear to require deeper semantic integration across heterogeneous abstractions. This observation aligns with the inherent complexity of emerging 6G scenarios that involve multi-domain coordination and distributed cognition.

6) *Scaling Sensitivity Across Capability Domains*: Table V presents the scaling sensitivity coefficients S_{G_j} computed between the smallest model (SmolLM2-135M, $N_{\min} = 0.135\text{B}$) and the largest model (Qwen2.5-7B, $N_{\max} = 7\text{B}$). The results reveal clear heterogeneity in how semantic capability classes benefit from parameter scaling. Intent & Policy Reasoning (G1) exhibits the highest sensitivity ($S_{G1} = 0.154$), indicating that multi-step intent alignment and consistency under uncertainty improve most strongly with increasing model capacity. Distributed Intelligence & Emerging 6G Use Cases (G5) also shows pronounced scaling dependence ($S_{G5} = 0.131$), reflecting the complexity of reasoning required for federated learning orchestration, Integrated Sensing and Communication (ISAC), and digital twin coordination. In contrast, Trust, Security & Service-Level Agreement (SLA) Awareness (G3) demonstrates the lowest sensitivity ($S_{G3} = 0.104$), suggesting that these tasks rely less on raw parameter scaling and more on structured policy reasoning and alignment mechanisms. Network Slicing & Resource Management (G2) and AI-Native Networking & Agentic Control (G4) occupy intermediate positions, exhibiting steady but moderate scaling gains. These results quantitatively confirm the heterogeneous scaling elasticity observed across semantic domains.

C. Inference Cost and Efficiency Profiling

Table VI reports single-query inference profiling across all evaluated LLMs under deterministic decoding. Latency and throughput scale nonlinearly with parameter count: ultra-compact models (135M–350M) achieve sub-150 ms latency and the lowest memory footprints, while 7B–8B models incur 300–550 ms latency and substantially higher compute cost. Peak VRAM does not strictly follow parameter size, with certain architectures exhibiting disproportionately large memory footprints, indicating implementation-dependent overheads. Throughput generally declines beyond the 1–3B regime, reflecting diminishing efficiency gains at larger scales. Theoretical forward-pass FLOPs per query increase approximately

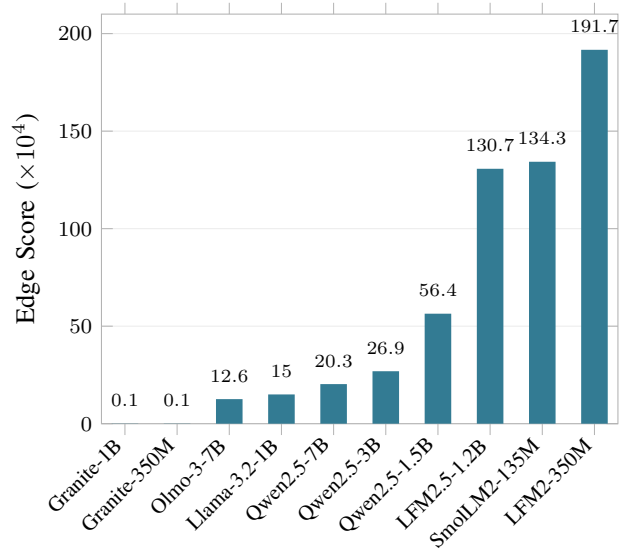


Fig. 7. Edge Score ranking of evaluated LLMs on 6G-Bench. Edge Score is defined as $ES = A_1 / (L \cdot M)$, where A_1 is deterministic accuracy, L is latency (ms), and M is peak VRAM (GB). Scores are scaled by 10^4 ; higher values indicate better semantic reliability per unit edge resource.

linearly with model size, ranging from 1.69 TF (135M) to over 100 TF (8B). These results highlight a clear trade-off between semantic capability gains and inference cost, suggesting that mid-scale models (1.5–3B) provide a favorable balance between stability and deployability in resource-constrained 6G edge environments.

D. Design Implications for Edge Deployment

The heterogeneous scaling behavior across groups, combined with the global trends in Table IV, the inference cost profiling in Table VI, and the deployment-aware efficiency ranking in Figure 7, has immediate consequences for the design of AI-native 6G architectures. Together, these results expose a joint capability–efficiency frontier: while larger models improve deterministic stability and cross-domain reasoning, they impose sharply increasing latency, memory, and compute burdens that directly constrain the feasibility of edge deployment. The Edge Score explicitly quantifies this trade-off, revealing that semantic reliability per unit edge resource does not scale monotonically with parameter count.

First, the sharp improvement in deterministic accuracy A_1 and contraction of the instability gap Δ_5 between 1B and 1.5B parameters suggest that this region constitutes a critical stability threshold for many semantic control tasks. For intent reasoning (G1), agentic control (G4), and distributed intelligence (G5), models below this threshold frequently exhibit fragmented or inconsistent behavior across turns, whereas mid-scale models (1.5–3B) provide substantially more reliable control trajectories. However, as shown by the Edge Score ranking, not all models within this region are equally deployment-efficient; architectural efficiency and memory footprint materially affect edge suitability.

Second, the moderate scaling sensitivity and earlier saturation observed in network slicing and resource management

TABLE VI
SINGLE-QUERY INFERENCE PROFILE (MEAN \pm STD) FOR LLMs EVALUATED ON 6G-BENCH.

Model	Params (B)	Peak VRAM (GB)	Latency (ms)	Throughput (tok/s)	FLOPs/query (TF)
HuggingFaceTB/SmolLM2-135M-Instruct	0.135	0.331 \pm 0.000	50.4 \pm 100.8	68.7 \pm 15.8	1.692 \pm 0.000
LiquidAI/LFM2-350M	0.354	0.137 \pm 0.001	136.3 \pm 154.1	75.1 \pm 15.3	4.375 \pm 0.000
ibm-granite/granite-4.0-h-350m	0.340	16.194 \pm 0.000	1814.7 \pm 128.7	3.9 \pm 0.2	4.074 \pm 0.000
meta-llama/Llama-3.2-1B-Instruct	1.236	2.481 \pm 0.000	100.1 \pm 111.2	89.0 \pm 18.1	13.688 \pm 0.000
LiquidAI/LFM2.5-1.2B-Instruct	1.170	0.266 \pm 0.002	152.5 \pm 153.0	64.7 \pm 12.9	14.444 \pm 0.000
ibm-granite/granite-4.0-h-1b	1.462	20.371 \pm 0.000	3161.3 \pm 63.3	2.2 \pm 0.0	17.495 \pm 0.000
Qwen/Qwen2.5-1.5B-Instruct	1.544	0.449 \pm 0.001	209.7 \pm 179.1	40.1 \pm 8.9	17.654 \pm 0.000
Qwen/Qwen2.5-3B-Instruct	3.086	0.874 \pm 0.000	273.9 \pm 181.1	29.2 \pm 6.0	35.291 \pm 0.000
allenai/Olmo-3-7B-Instruct	7.298	1.336 \pm 0.000	386.3 \pm 180.1	19.5 \pm 3.2	87.357 \pm 0.000
Qwen/Qwen2.5-7B-Instruct	7.616	1.028 \pm 0.000	338.7 \pm 202.3	23.0 \pm 4.0	87.092 \pm 0.000
LiquidAI/LFM2-8B-A1B	8.340	1.275 \pm 0.000	552.2 \pm 295.8	15.9 \pm 2.9	102.931 \pm 0.000

Notes: Results are mean \pm standard deviation over $R = 20$ runs. Prompt length: 2049 input tokens; generated tokens: 8. Measurements collected with deterministic decoding (temperature=0), bf16, no quantization. All results correspond to single-GPU execution.

(G2) and trust and security (G3) indicate that these domains can be served by smaller models without catastrophic degradation. Tasks such as slice selection (T4), compute placement (T7), trust-aware offloading (T9), and identity onboarding (T18) remain partially tractable in the sub-1B regime. Importantly, Figure 7 demonstrates that well-optimized ultra-compact models can dominate the edge-efficiency frontier, achieving superior reliability-to-resource ratios despite lower absolute accuracy. This suggests that compact models can be positioned close to the radio and edge, handling localized resource and trust decisions, while more complex intent and coordination reasoning is delegated to mid-scale models higher in the control hierarchy.

Third, the decreasing log-scale reasoning efficiency $\eta(N)$ and the Edge Score frontier jointly highlight a key trade-off: although larger models achieve higher absolute accuracy, they do so at lower deployment-normalized efficiency. In practice, this argues for a tiered design rather than uniform scaling. A plausible pattern is:

- ultra-compact models (≤ 350 M) embedded at RAN and MEC nodes to provide fast, approximate reasoning for G2/G3-type decisions and low-risk advisory functions;
- mid-scale models (1.5–3B) anchored at regional or core control-plane locations to handle stability-critical G1, G4, and G5 decisions under deterministic decoding; and
- optional 7B-class models in centralized orchestration roles, where marginal gains in robustness and cross-domain synthesis justify higher resource consumption.

This capability- and tier-aware partitioning aligns naturally with current standardization trends toward hierarchical control and distributed intelligence. The Edge Score analysis reinforces that the optimal deployment strategy is not to maximize parameter scale, but to identify the minimal capacity that achieves stable deterministic reasoning under edge resource constraints. Accordingly, the design question for AI-native networks should not be “how large a model can be deployed,” but “which semantic capabilities must be hosted at which tier, and what is the minimal stable capacity required for each.”

E. Limitations and Reliability Concerns

While the focus of this study is on deterministic reliability and scaling regimes, the results also surface important reli-

ability considerations. The instability gap Δ_5 shows that in the ultra-compact regime, correct reasoning trajectories are often present among stochastic samples but are not consistently selected by deterministic decoding. For safety-critical functions such as intent feasibility checks (T1), conservative continuation (T12), SLA violation prediction (T10), or security incident response (T30), this gap is problematic: stochastic recoverability does not translate into operational safety.

Even at 3B and 7B, Δ_5 remains non-zero, indicating residual divergence between exploration and exploitation. In practice, this motivates combining mid- to large-scale models with complementary mechanisms such as policy verifiers, rule-based filters, and constrained decoding. Domains with lower scaling elasticity but high safety impact — particularly G3 — are well suited to such hybrid designs, in which compact semantic reasoning is wrapped in explicit policy logic.

Finally, although our model set spans multiple organizations and architectures, it is not exhaustive. Differences in training data, alignment pipelines, and optimization objectives introduce architecture-dependent deviations from pure log-linear scaling. Likewise, 6G-Bench captures a broad but still bounded set of tasks aligned with current standardization discussions. As AI-native networks evolve toward more complex, multi-modal, and adversarial environments, further work will be needed to reassess stability thresholds and domain sensitivities. Nonetheless, the regimes and patterns identified here provide a concrete starting point for designing capability-aware, resource-constrained semantic control layers in AI-native 6G systems.

V. CONCLUSION

This paper presented the first systematic scaling study of small and tiny language models (135M–7B parameters) for network-level semantic reasoning in AI-native 6G systems using the 6G-Bench standardization-aligned framework. Our results demonstrate that deterministic reasoning reliability scales non-uniformly with model size, revealing a pronounced stability transition in the 1–1.5B parameter range and diminishing marginal returns beyond 3B parameters. The contraction of the instability gap from 0.365 in the ultra-compact regime to 0.031 at 7B indicates convergence between stochastic exploration and deterministic inference, a prerequisite for safety-

critical control under zero-trust and SLA-constrained environments. Moreover, heterogeneous scaling elasticity across capability domains shows that intent reasoning and distributed intelligence tasks are strongly scale-sensitive, whereas trust and structured resource management exhibit earlier saturation. These findings establish that mid-scale models (1.5–3B) achieve a critical balance between computational footprint and deterministic stability, providing quantitative guidance for deploying LLM-based AI agents across hierarchical 6G tiers—from edge-native RAN and MEC nodes to centralized orchestration layers. Ultimately, our study reframes model scaling not as a race toward ever-larger architectures, but as a principled search for the minimal stable capacity required to support reliable semantic control in AI-native, RIS-enabled, THz-capable, and quantum-secure 6G networks.

REFERENCES

- [1] E. A. Anowr, M. Nashaat, M. I. Ismail, M. A. Mohamed, M. M. Fouda, and H. M. Abdel-Atty, "F-iran: Performance analysis of 6g fog intelligent radio access network," *IEEE Open Journal of the Communications Society*, 2025.
- [2] 3GPP, "Study on 6g use cases and service requirements," 3rd Generation Partnership Project (3GPP), Tech. Rep. TR 22.870, 2025.
- [3] O-RAN Alliance e.V., "Generative ai use cases and requirements on 6g network," O-RAN Alliance, Research Report, Jan 2025, next Generation Research Group (nGRG). [Online]. Available: <https://www.o-ran.org/research-reports/generative-ai-use-cases-and-requirements-on-6g-network>
- [4] ETSI, *Multi-access Edge Computing (MEC); Framework and Reference Architecture*, European Telecommunications Standards Institute (ETSI) Std. GS MEC 003 V3.1.1, Mar. 2022.
- [5] C. Yang, H. Huang, A. Akhavain, F. Liu, X. An, W. Xing, J. Li, A. Wang, and W. Yang, "Requirements and enabling technologies of agent protocols for 6g networks," Internet Engineering Task Force (IETF), Internet-Draft draft-hw-ai-agent-6g-00, Jul. 2025. [Online]. Available: <https://www.ietf.org/archive/id/draft-hw-ai-agent-6g-00.html>
- [6] E. Hossain and A. Vera-Rivera, "6g cellular networks: Mapping the landscape for the imt-2030 framework," *IEEE Transactions on Technology and Society*, 2025.
- [7] S. Ye, M. Xiao, M.-W. Kwan, Z. Ma, Y. Huang, G. Karagiannidis, and P. Fan, "Extremely large aperture array (elaa) communications: Foundations, research advances and challenges," *IEEE Open Journal of the Communications Society*, vol. 5, pp. 7075–7120, 2024.
- [8] Y. Lu, J. Zhang, E. Shi, P. Zhang, D. W. K. Ng, D. Niyato, and B. Ai, "Energy-efficient ris-aided cell-free massive mimo systems: Application, opportunities, and challenges," *IEEE Wireless Communications*, 2025.
- [9] B. Banerjee *et al.*, "6g phy: Insights from 6g-anna research initiative," *IEEE Open Journal of the Communications Society*, 2026.
- [10] S. Sharif, F. Khandaker, M. Naeem, and W. Ejaz, "Resource optimization for semantic communication in 6g networks: A survey," *IEEE Open Journal of the Communications Society*, 2026.
- [11] T. N. Turnip, B. Andersen, and C. Vargas-Rosales, "Towards 6g authentication and key agreement protocol: A survey on hybrid post quantum cryptography," *IEEE Communications Surveys & Tutorials*, 2025.
- [12] K. Gogineni, A. Suvizi, and G. Venkataramani, "Llms on a budget: System-level approaches to power-efficient and scalable fine-tuning," *IEEE Open Journal of the Computer Society*, 2025.
- [13] M. A. Ferrag, A. Lakas, and M. Debbah, " α^3 -bench: A unified benchmark of safety, robustness, and efficiency for llm-based uav agents over 6g networks," *arXiv preprint arXiv:2601.03281*, 2026.
- [14] J. Hoffmann, S. Borgeaud, A. Mensch, E. Buchatskaya, T. Cai, E. Rutherford, D. Casas, L. A. Hendricks, J. Welbl, A. Clark *et al.*, "Training compute-optimal large language models," *arXiv preprint arXiv:2203.15556*, vol. 10, 2022.
- [15] J. Kaplan, S. McCandlish, T. Henighan, T. B. Brown, B. Chess, R. Child, S. Gray, A. Radford, J. Wu, and D. Amodei, "Scaling laws for neural language models," *arXiv preprint arXiv:2001.08361*, 2020.
- [16] J. Wei, Y. Tay, R. Bommasani, C. Raffel, B. Zoph, S. Borgeaud, D. Yogatama, M. Bosma, D. Zhou, D. Metzler *et al.*, "Emergent abilities of large language models," *arXiv preprint arXiv:2206.07682*, 2022.
- [17] M. A. Ferrag, A. Lakas, and M. Debbah, "6g-bench: An open benchmark for semantic communication and network-level reasoning with foundation models in ai-native 6g networks," *arXiv preprint arXiv:2602.08675*, 2026.
- [18] J. W. Rae, S. Borgeaud, T. Cai, K. Millican, J. Hoffmann, F. Song, J. Aslanides, S. Henderson, R. Ring, S. Young *et al.*, "Scaling language models: Methods, analysis & insights from training gopher," *arXiv preprint arXiv:2112.11446*, 2021.
- [19] L. B. Allal, A. Lozhkov, E. Bakouch, G. M. Blázquez, G. Penedo, L. Tunstall, A. Marafioti, H. Kydliček, A. P. Lajarín, V. Srivastav *et al.*, "Smollm2: When smol goes big—data-centric training of a small language model," *arXiv preprint arXiv:2502.02737*, 2025.
- [20] IBM Research, "Granite 4.0 nano language models," <https://github.com/ibm-granite/granite-4.0-nano-language-models>, 2025, accessed: 2026-02-19.
- [21] L. AI, "Lfm2 technical report," *arXiv preprint arXiv:2511.23404*, 2025.
- [22] A. Grattafiori, A. Dubey, A. Jauhri, A. Pandey, A. Kadian, A. Al-Dahle, A. Letman, A. Mathur, A. Schelten, A. Vaughan *et al.*, "The llama 3 herd of models," *arXiv preprint arXiv:2407.21783*, 2024.
- [23] Q. Team, "Qwen2.5: A party of foundation models," September 2024. [Online]. Available: <https://qwenlm.github.io/blog/qwen2.5/>
- [24] A. Yang *et al.*, "Qwen2 technical report," *arXiv preprint arXiv:2407.10671*, 2024.
- [25] T. Olmo *et al.*, "Olmo 3," *arXiv preprint arXiv:2512.13961*, 2025.